Tunable optical metamaterial based on liquid crystal-gold nanosphere composite

R. Pratibha,[1,2,3], K. Park[1], I. I. Smalyukh[2]and W. Park[1*]

[1]*Department of Electrical and Computer Engineering, University of Colorado, Boulder, Colorado, USA*
[2]*Department of Physics, University of Colorado, Boulder, Colorado, USA*
[3]*Raman Research Institute, C.V. Raman Avenue, Bangalore,560 080,India*
**WonPark@colorado.edu*

Abstract: Effect of the surrounding anisotropic liquid crystal medium on the surface plasmon resonance (SPR) exhibited by concentrated suspensions of gold nanospheres has been investigated experimentally and compared with the Mie scattering theory. The observed polarization-sensitive SPR and the red-shift in the SPR wavelength with increasing concentration of the gold nanospheres in the liquid crystal matrix have been explained using calculations based on the Maxwell Garnet effective medium theory. Agglomeration of the gold nanospheres that could also lead to such a red-shift has been ruled out using Atomic force microscopy study of thin nanoparticle-doped smectic films obtained on solid substrates. Our study demonstrates feasibility of obtaining tunable optical bulk metamaterials based on smectic liquid crystal - nanoparticle composites.

OCIS codes: (160.3918) Metamaterials; (160.3710) Liquid crystals; (160.4236) Nanomaterials.

References and links

1. Y. Wang, "Voltage induced color selective absorption with surface plasmons," Appl. Phys. Lett. **67**(19), 2759–2761 (1995).
2. X. Wang, and K. Do-Hoon, D. H. Werner, I. C. Khoo, A.V. Kildishev and V. M. Shalaev, "Tunable optical negative-index metamaterials employing anisotropic liquid crystals," Appl. Phys. Lett. **91**, 1–3 (2007).
3. G. Mie, "Beiträge zur Optik trüber Medien, speziell kolloidaler Metallösungen," Ann. Phys. **330**(3), 377–445 (1908).
4. U. Kreibig, M. Völlmer, *Optical Properties of Metal Clusters* (Springer-Verlag, Berlin 1995).
5. S. Kubo, A. Diaz, Y. Tang, T. S. Mayer, I. C. Khoo, and T. E. Mallouk, "Tunability of the refractive index of gold nanoparticle dispersions," Nano Lett. **7**(11), 3418–3423 (2007).
6. P. G. De Gennes, and J. Prost, *The Physics of Liquid Crystals* (Clarendon Press, Oxford 1995).
7. S. Chandrasekhar, *Liquid Crystals* (Cambridge University Press, Cambridge 1992).
8. I. C. Khoo, D. H. Werner, X. Liang, A. Diaz, and B. Weiner, "Nanosphere dispersed liquid crystals for tunable negative-zero-positive index of refraction in the optical and terahertz regimes," Opt. Lett. **31**(17), 2592–2594 (2006).
9. R. Pratibha, W. Park, and I. I. Smalyukh are preparing a manuscript to be called "Elasticity and layer structure stabilized colloidal nanoparticle dispersions in lamellar liquid crystals"
10. V. Yannopapas, and A. Moroz, "Negative refractive index metamaterials from inherently non-magnetic materials for deep infrared to terahertz frequency ranges," J. Phys. Condens. Matter **17**(25), 3717–3734 (2005).
11. J. J. Storhoff, R. Elghanian, R. C. Mucic, C. A. Mirkin, and R. L. Letsinger, "One-Pot Colorimetric Differentiation of Polynucleotides with Single Base Imperfections Using Gold Nanoparticle Probes," J. Am. Chem. Soc. **120**(9), 1959–1964 (1998).
12. C. F. Bohren, and D. R. Huffman, *Absorption and Scattering of Light by Small Particles* (New York: Wiley-Interscience1983).
13. P. B. Johnson, and R. W. Christy, "Optical Constants of the Noble Metals," Phys. Rev. B **6**(12), 4370–4379 (1972).
14. G. M. Koenig, Jr., M.-V. Meli, J. S. Park, J. J. de Pablo, and N. L. Abbott, "Coupling of the Plasmon resonances of chemically functionlized gold nanoparticles to local order in thermotropic liquid crystals," Chem. Mater. **19**(5), 1053–1061 (2007).
15. H. Stark, "Physics of colloidal dispersions in nematic liquid crystals," Phys. Rep. **351**(6), 387–474 (2001).
16. P. Poulin, H. Stark, T. C. Lubensky, and D. A. Weitz, "Novel colloidal interactions in anisotropic fluids," Science **275**(5307), 1770–1773 (1997).

#116095 - $15.00 USD Received 26 Aug 2009; revised 4 Oct 2009; accepted 4 Oct 2009; published 13 Oct 2009

17. R. W. Ruhwandl, and E. M. Terentjev, "Long-range forces and aggregation of colloidal particles in a nematic liquid crystal," Phys. Rev. E Stat. Phys. Plasmas Fluids Relat. Interdiscip. Topics **55**(3), 2958–2961 (1997).
18. F. S. Y. Yeung, Y. L. J. Ho, Y. W. Li, and H. S. Kwok,"Liquid crystal alignment layer with controllable anchoring energies," J. Display Tech **4**(1), 24–27 (2008).
19. S. Y. Park, and D. Stroud, "Surface-enhanced plasmon plitting in a liquid crystal-coated gold nanoparticle," Phys. Rev. Lett. **94**(21), 217401 (2005).
20. J. Müller, C. Sonnichsen, H. von Poschinger, G. von Plessen, T. A. Klar, and J. Feldmann, "Electrically controlled light scatterring with single metal nanoparticles," Appl. Phys. Lett. **81**(1), 171–173 (2002).
21. S. Y. Park, and D. Stroud, "Splitting of surface plasmon frequencies of metal particles in a nematic liquid crystal," Appl. Phys. Lett. **85**(14), 2920–2922 (2004).
22. P. Sens, and M. S. Turner, "Inclusions in thin smectic films", J. Phys, II France **7**(12), 1855–1870 (1997).
23. M. S. Turner, and P. Sens, "Interactions between particulate inclusions in a smectic-A liquid crystal," Phys. Rev. **55**, R1275–R1278 (1997).
24. C. D. Santangelo, and R. D. Kamien, "Bogomol'nyi, Prasad, and Sommerfield Configurations in smectics," Phys. Rev. Lett. **91**(4), 045506 (2003).
25. G. Liao, I. I. Smalyukh, J. R. Kelly, O. D. Lavrentovich, and A. Jakli, "Electrorotation of colloidal particles in liquid crystals," Phys. Rev. E Stat. Nonlin. Soft Matter Phys. **72**, 1–5 (2005).

1. Introduction

Research on metamaterials having tunable optical properties at the required spectral range, is of great current interest because of numerous potential applications. A recently proposed technique to obtain such materials is to have composites made of tunable materials. Metal nanostructures which exhibit strong plasmon resonance and liquid crystals possessing order and fluidity and having the capacity to respond to external fields that can influence their structure and properties, offer a very attractive combination. There have been some reports of combining liquid crystals and plasmonic metals involving techniques requiring complex fabrication processes. One of the earliest experiments used a silver film and liquid crystal (LC) interface and showed that a shift in the surface plasmon resonance frequency could be obtained by a voltage induced change in the refractive index of the liquid crystal [1]. A more recent design fabrication to obtain tunable negative index materials suggests the use of nanostrip pairs of silver separated by a liquid crystal layer [2]. The refractive index tunability is achieved either by changing the orientation of the liquid crystal molecules by means of an external field or by varying the temperature.

The recent surge of activity in the field of nanoparticle synthesis has opened up the possibility of incorporating these particles to form functional composites. A theoretical treatment of plasmon resonance absorption of gold colloids based on Maxwell's electromagnetic theory has been given by Gustav Mie [3]. The strong absorption band is exhibited by noble metal nanoparticles in the visible region when the photon frequency is resonant with the collective oscillation of the conduction electrons and is known as the surface plasmon resonance. It is the most striking optical property of metallic nanoparticles and forms the basis for both understanding various coupling interactions between the nanoparticles and in technological applications. The resonance frequency is related to the metal, the size and shape of the nanoparticles and the refractive index of the surrounding medium [4]. These effects combine to extend the tunability of the optical properties of such systems. Studies on gold colloids in various organic solvents are in agreement with the Mie scattering theory. Tunability as a function of dielectric constant of the host media and volume fraction of gold spheres has been demonstrated experimentally in dispersions of metal spheres and metal shell-dielectric core nanoparticles in hydrocarbons and also modeled using Mie scattering theory [5].

The nematic liquid crystal formed by rigid rod-like molecules is characterized by a long range orientational order but no translational order [6,7]. The principle axes of the molecules are oriented on an average along a direction called the *director* which is apolar in nature. In the smectic phase, in addition to the orientational order a one-dimensional translational order is present resulting in a layered arrangement of the molecules [6,7]. In the smectic A phase

#116095 - $15.00 USD Received 26 Aug 2009; revised 4 Oct 2009; accepted 4 Oct 2009; published 13 Oct 2009

the molecules are parallel to the layer normal with a liquid-like arrangement within the layers. Usually the nematic and smectic A phases made of rod-like molecules are uniaxial.

The possibility of obtaining refractive index tunability in a composite system consisting of a nematic liquid crystal with dispersed core-shell nanospheres has been suggested theoretically [8]. Combination of the relative permittivities of the particles and the field – induced permittivity change in the liquid crystal gives rise to a tunable effective refractive index of the composite medium. However, no systematic experimental studies of such composites have been reported.

In this paper we describe our experimental studies of plasmonic effects exhibited by stable concentrated dispersions of gold nanoparticles in smectic liquid crystals [9]. The effect of the surrounding anisotropic liquid crystal medium on the experimentally observed surface plasmon resonance wavelength ($\lambda_{\max}^{SPR}$) has been compared with the Mie scattering theory. The progressive red-shift in $\lambda_{\max}^{SPR}$ observed with increasing volume fraction of the nanoparticles in the liquid crystal matrix is in agreement with calculations based on the extended Maxwell Garnet effective medium theory [10] and is further supported by the study of surface profiles of thin nanoparticle-doped smectic films.

2. Experimental techniques and materials

The absorption spectra were recorded using the Ocean Optics miniature fiber optic spectrometer (USB2000) in conjunction with a polarizing microscope. Atomic force microscopy studies were carried out in the tapping mode using Nanoscope III AFM from digital Instruments.

The liquid crystalline compound 4-*n*- octyl 4′-cyanobiphenyl (8CB, from Frinton Labs) which exhibits the phase sequence Cr 21 SmA 32 N 40.5 I (°C) has been used. The synthesis of gold nanoparticles was carried out by the conventional solution-based technique [11]. Briefly, auric acid ($HAuCl_4$) was first dissolved in deionized water and a reducing agent such as sodium citrate was subsequently added to initiate homogeneous precipitation of metal nanoparticles. The pH and temperature were carefully controlled in order to obtain good size distribution. Spherical gold nanoparticles of mean diameter 14nm as measured with SEM were initially formed in aqueous medium. In order to improve the efficiency of distribution and stabilization in the liquid crystalline medium, the nanoparticles were first coated with the amphiphilic, nonionic polymer poly (*N*-vinyl-2-pyrrolidone) (PVP 10 from Aldrich). The nanoparticles were then transferred from the aqueous medium to the organic solvent ethyl alcohol, to facilitate better compatibility with the thermotropic liquid crystal used in our studies. Measured amount of the suspension was added to the liquid crystalline compound in order to obtain specific volume fractions of the PVP coated gold nanoparticles (GNPs) in the liquid crystal. The temperature was maintained at 24°C such that the liquid crystal is in the smectic A phase and the mixture of GNPs in ethyl alcohol and liquid crystal continuously stirred for about 5 hours. After evaporation of most of the ethyl alcohol the solution was filled into cells made of rubbed glass plates. The remaining alcohol was allowed to evaporate over a few hours. As the alcohol evaporated, well aligned regions of smectic A liquid crystal with a planar alignment having an overall orientation of the *director* along the rubbing direction were obtained. The absorption spectra in the smectic A phase were recorded at 24°C for all samples.

3. Results and discussion

The absorption spectrum with the PVP coated gold nanoparticles in ethyl alcohol was first recorded before addition of the liquid crystal. The wavelength corresponding to the absorption maximum was found to occur at 522nm. After the addition of this suspension to the liquid crystal and subsequent evaporation of the ethyl alcohol as described above, the optical textures exhibited by the liquid crystalline dispersions in the smectic A phase were observed

#116095 - $15.00 USD Received 26 Aug 2009; revised 4 Oct 2009; accepted 4 Oct 2009; published 13 Oct 2009

under the polarizing microscope using the planar aligned cells. Uniform regions with planar alignment of smectic A liquid crystal were obtained. The optical textures as observed under the polarizing microscope were very similar to that obtained with pure 8CB when the concentration of GNPs was low as shown in Fig. 1a. However with a relatively large volume fraction (Φ) ~0.5 of the GNPs, the texture exhibited an intense green color but with the focal conic like features of the smectic A phase, remaining intact as shown in Fig. 1b.

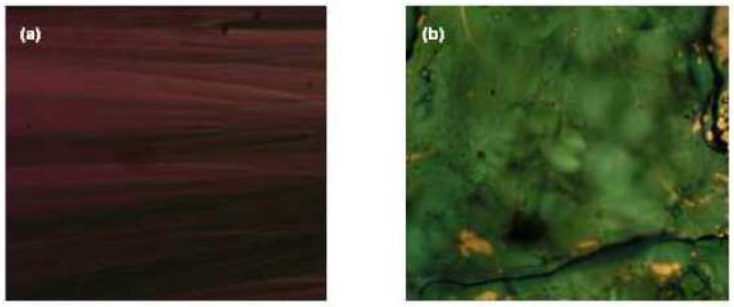

Fig. 1. Focal conic texture observed in the smectic A phase of the LC-GNP dispersions viewed between crossed polarizers, (a) Φ = 0.21 and (b) Φ =0.54.

Optical absorption spectra were then recorded using the planar aligned cells. The spectra show that there is a progressive shift of $\lambda_{\max}^{SPR}$ to longer wavelengths with increasing volume fraction of the GNPs. For the purpose of illustration we have shown in Fig. 2 the spectra for dispersions with Φ = 0.21 and Φ = 0.54 of GNPs in comparison to the spectrum obtained with the GNPs suspended in ethyl alcohol.

When the concentration of the GNPs is small the absorbance is also low leading to a marked difference in the peak absorbances for samples with Φ = 0.21 and Φ = 0.54. Though there should be a slight change in $\lambda_{\max}^{SPR}$ due to the change in the host dielectric medium from ethyl alcohol to the smectic liquid crystal, the shift is mainly due to the coupling between SPR from individual particles which we later describe using the effective medium theory.

We first investigated the effect of an anisotropic medium surrounding the nanoparticles on the surface plasmon resonance wavelength. In the case of uniaxial liquid crystals the direction of the optic axis is along the *director*. Because of the anisotropic nature of the liquid crystal the velocity of propagation of a light beam polarized along the *director* is different from that propagating perpendicular to it. This results in two refractive indexes, n_e the extraordinary refractive index for a light wave propagating with electric vector parallel to the *director* and n_0 the ordinary refractive index for a light wave propagating perpendicular to the *director*. Therefore when the nanoparticles are covered by the anisotropic liquid crystalline medium the observed particle plasmon resonance depends on the angle between the *director* and the polarization of the incident light and is related with the relevant refractive index.

#116095 - $15.00 USD Received 26 Aug 2009; revised 4 Oct 2009; accepted 4 Oct 2009; published 13 Oct 2009

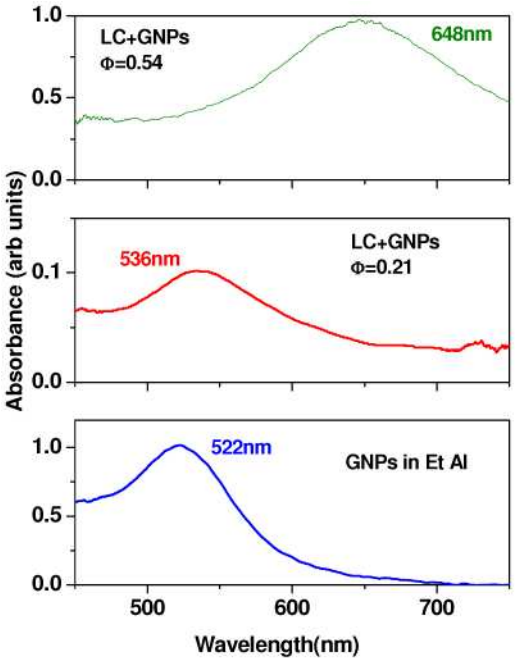

Fig. 2. Optical absorption spectra obtained with GNPs suspended in ethyl alcohol before addition of the liquid crystal and LC-GNP dispersions with Φ = 0.21 and Φ = 0.54.

We have performed absorption measurements on planar aligned samples with a light beam polarized along (P=0°), and perpendicular (P=90°) to the average orientation of the *director* in the bulk of the sample. The two orientations of the polarizer P=0° and P=90° correspond to the refractive indexes n_e and n_0 of the liquid crystal, respectively. Taking the example of a sample with Φ =0.23 a difference of ~13 nm in $\lambda_{\max}^{SPR}$ could be observed for P=0° and P=90°, with the wavelength being red-shifted for P=0°, as shown in Fig. 3a.

The red shift is often observed if the average refractive index of the medium increases. This increase can be expected, as in our planar aligned samples when the light beam is polarized parallel to the *director* the refractive index would mainly correspond to the higher refractive index n_e. We have performed Mie scattering calculations [12] assuming isotropic materials with refractive indexes taken to be $n=1.7$ and $n=1.5$, comparable to the extraordinary (n_e) and ordinary (n_0) refractive indexes of the liquid crystal 8CB used in our study. The experimentally determined refractive index of gold was used in these calculations [13]. As shown in Fig. 3b, a difference of 21nm is obtained in $\lambda_{\max}^{SPR}$ for calculations with $n=1.7$ and $n=1.5$ with the wavelength being higher when $n=1.7$ is considered.

#116095 - $15.00 USD Received 26 Aug 2009; revised 4 Oct 2009; accepted 4 Oct 2009; published 13 Oct 2009

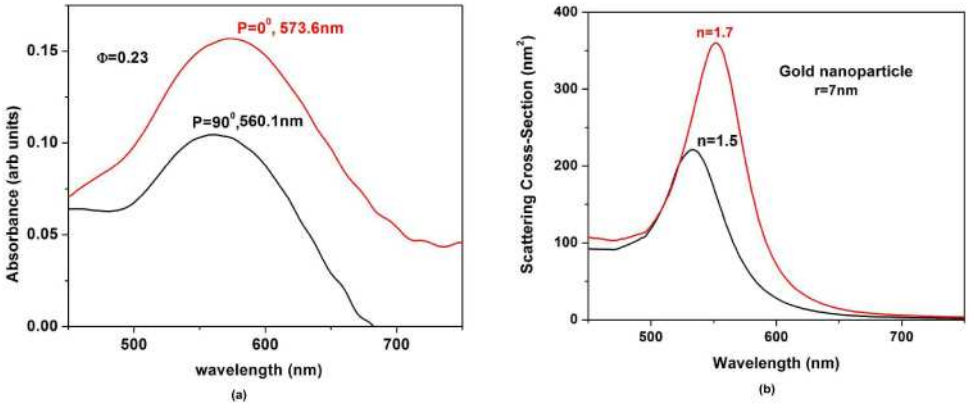

Fig. 3. (a) Optical spectra obtained with comparable volume fractions of GNPs (a) from experiment and (b) from calculations based on Mie scattering theory.

Our calculations account for the observed red shift. However the experimental peaks are broader and the difference in wavelength obtained with P=0° and P=90° is smaller than that obtained from calculations. One of the reasons for the peak broadening might be the polydispersity of particle sizes. Our TEM studies revealed that the particle sizes varied from 12 to 22 nm. The other effect, which is likely to play a more important role, is the local order of the liquid crystal around the suspended particles which is affected by the surface of the particle as a result of the elastic distortions associated with the liquid crystal and the anchoring energy between the surfaces of the particles and the liquid crystal. Previous studies on immobilized gold nanoparticles that have been chemically functionalized with organic monolayers which give different types of orientations of the liquid crystal *director* near the surface of the particles show that the localized surface plasmon resonance can vary depending on the nature of the organic monolayer [14]. If the anchoring is strong the boundary conditions at the surface of the particle can impart a specific orientation to the *director* resulting in topological defects [15–17]. But if the anchoring is weak the *director* distortion is not much and can be close to the orientation in the far field of the particles as imposed by the rubbing action. The polymer PVP that we are using as a capping agent is known to be a non-aligning polymer with weak surface anchoring properties [18]. Therefore in the dispersions used in our study, the layered structure and the liquid crystal *director* (orthogonal to the layers) in the close vicinity of the particles can be uniform or adopt configurations as shown in Fig. 4a and 4b.

In the dispersed medium, as either of the configurations can be adopted, there can be variations from particle to particle in the observed shifts in $\lambda_{\max}^{SPR}$ as the refractive index in the region surrounding the particles is different, resulting in a broadening of the peaks. In fact calculations on a single gold nanoparticle coated with a thin layer of nematic liquid crystal and considering three possible orientations of the *director* at the surface of the nanoparticle surface have shown that the splitting of surface plasmon frequency depends on the deformation near the surface which can even be influenced by the thickness of the coating [19]. Particle – particle interactions also become important in influencing the *director* orientations. These combined effects smear out the distinction between $\lambda_{\max}^{SPR}$ obtained with P =0and P=90°. Therefore in reality it would be more appropriate to consider an effective refractive index for the liquid crystal matrix in the calculations. In another study, changes in surface plasmon frequency have been investigated in a planar aligned liquid crystal cell with

#116095 - $15.00 USD Received 26 Aug 2009; revised 4 Oct 2009; accepted 4 Oct 2009; published 13 Oct 2009

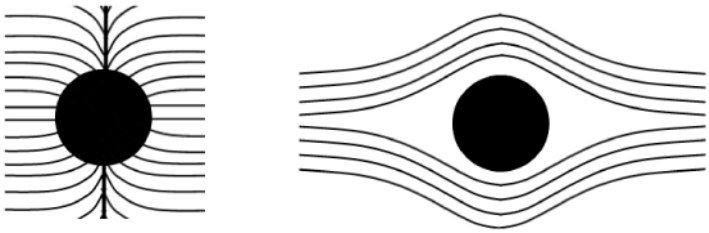

Fig. 4. Schematic representation of the smectic layers around the nanoparticles when the *director* orientation at the surface is (a) tangential and (b) radial.

embedded gold nanoparticles which adhere onto the polyimide layer used to align the liquid crystal [20]. The orientation of the liquid crystal *director* is varied by application of an electric field. The authors find that the particle plasmon resonance associated with the refractive index n_e exhibits a blue shift related with the lowering of the refractive index as the molecules reorient along the field direction. But they also observe changes in the particle plasmon resonance associated with n_0 which is not expected. The authors surmise that other factors like the local density of the liquid crystal molecules in the vicinity of the nanoparticles when the electric field is applied and alignment of the liquid crystal molecules at the surface of the nanoparticles could be important. This shows that even with adhered particles used in this study the result is not clear. In view of this, the splitting that we observe with the dispersions is quite reasonable. Other previous calculations of the splitting between the surface plasmon frequencies performed for a suspension of small metallic particles with uniform orientation conditions near the surface of the particle embedded in a nematic liquid crystal host show that the surface plasmon frequencies for light polarized parallel or perpendicular to the *director* varies by ~1 to 2% [21]. This is comparable to our experimental result which shows a difference of about 13nm between the $\lambda_{\max}^{SPR}$ obtained with P=0 and P=90°. So it is not surprising that we observe a smaller shift in the surface plasmon resonance splitting with the dispersed medium. An attempt to enhance the SPR splitting was made by improving the alignment of the sample by applying a magnetic field. But the shift in $\lambda_{\max}^{SPR}$ obtained with P=0° and P=90° shown in Fig. 5 was very similar to the shift obtained in flat cells made of rubbed glass plates. This indicates that the orientation of the liquid crystal *director* at the particle surface is more important than the overall alignment in the sample.

Mie scattering calculations show that the resonance wavelength shifts towards larger wavelengths as the particle size increases. Figure 6a and 6b show the dependence of scattering cross section as a function of wavelength for various particle sizes with background indexes $n=1.5$ and $n=1.7$. One possible reason for the red-shift observed in our samples with increasing concentration of the particles (Fig. 2) could be due to the agglomeration of the particles. Calculations show that a shift of the wavelength to ~630nm (for $n=1.5$) should correspond to a particle size of r ~60nm implying an agglomeration of approximately 600 of the r=7nm GNPs used in our study.

#116095 - $15.00 USD Received 26 Aug 2009; revised 4 Oct 2009; accepted 4 Oct 2009; published 13 Oct 2009

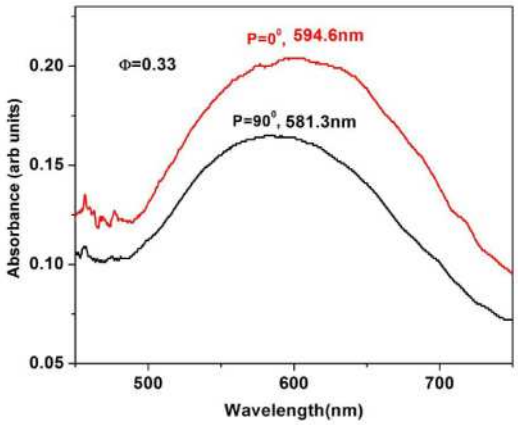

Fig. 5. Optical spectra obtained after the sample has been aligned under a magnetic field.

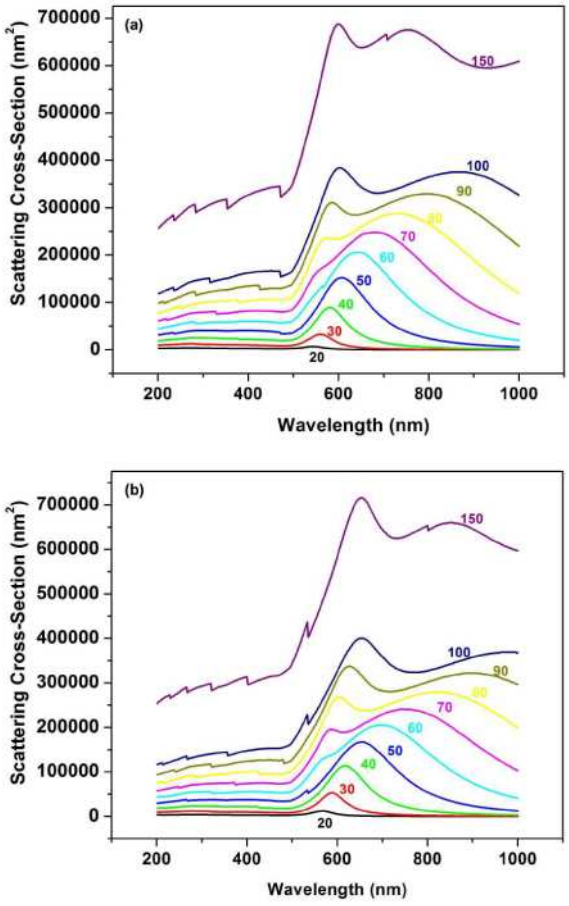

Fig. 6. Dependence of resonance wavelength on particle size ranging from r=20 to 150nm from Mie scattering calculations for refractive indexes (a) n =1.5 and (b) n =1.7.

#116095 - $15.00 USD Received 26 Aug 2009; revised 4 Oct 2009; accepted 4 Oct 2009; published 13 Oct 2009

In order to confirm the absence of agglomeration and also probe the distribution of the nanoparticles in the LC+GNPs samples we have used atomic force microcopy [9]. Inclusions immersed in smectic liquid crystals deform the layers resulting in a displacement of the layers along the layer normal [22–25]. When the LC-GNP dispersions are obtained in the form of thin (<100nm) films on Si substrates the nanoparticles give rise to such layer deformations resulting in raised hump like regions [9], with each hump corresponding to an individual nanoparticle, as shown in Fig. 7. The AFM images show that there is no severe agglomeration of the particles and they remain stabilized and well dispersed in the smectic A phase. The nanoparticles appear to be stabilized by repulsive interactions between particles within the same layer and limited mobility across the layers forming stable dispersions in the SmA phase [9].

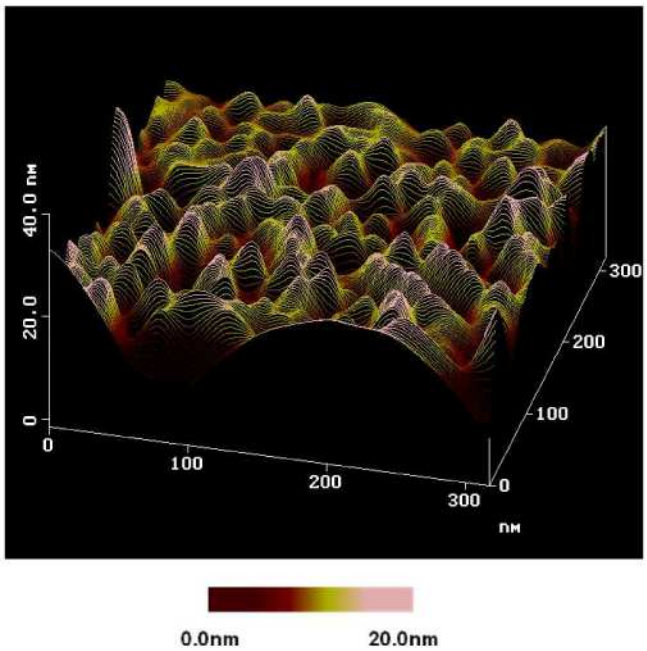

Fig. 7. AFM image of the hump like regions that correspond to layer deformations induced by the nanoparticles for a sample with Φ = 0.54.

The Maxwell Garnet effective medium theory can be used to characterize an inhomogeneous medium by treating the material as a homogeneous substance with an effective dielectric permittivity and effective magnetic permeability. These quantities depend on the properties of the constituents, as well as on their volume fractions and sizes. Following the extended Maxwell Garnett effective medium theory, we first calculated the polarizability of individual GNP using the Mie theory and then applied the Maxwell Garnett mixing rule to calculate the complex effective index for the composite structure [10]. From the imaginary part of the effective index we can obtain the expected absorption spectrum which can be directly compared with the experimental absorption spectrum.

In order to make comparisons with the effective medium theory a systematic study of the absorption profiles with increasing concentration of GNPs was carried out. Figure 8 shows a comparison between $\lambda_{\max}^{SPR}$ obtained from the effective medium calculations and that obtained experimentally from absorption measurements, as a function of increasing volume fraction. A reasonably good agreement was observed between the trend obtained from simulations and experiment with $\lambda_{\max}^{SPR}$ progressively increasing with increase in volume fraction of the GNPs.

#116095 - $15.00 USD Received 26 Aug 2009; revised 4 Oct 2009; accepted 4 Oct 2009; published 13 Oct 2009

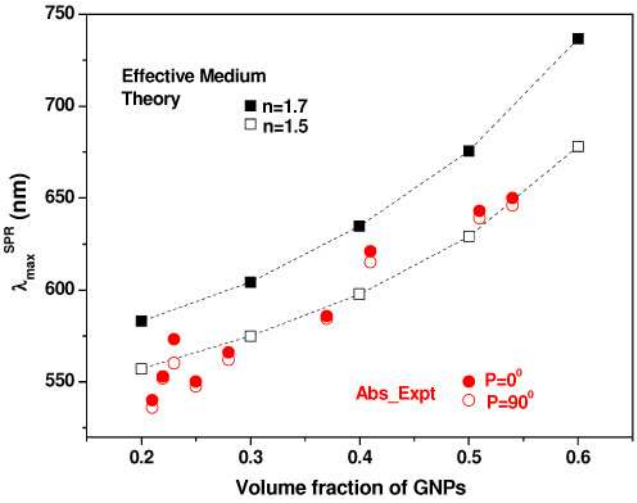

Fig. 8. Comparison of the surface plasmon resonance wavelength for different volume fraction of GNPs from effective medium calculations (dotted line drawn as guide to the eye) and from experimental absorption spectra obtained with polarizer P=0° and P=90°.

Due to reasons mentioned earlier the shift in $\lambda_{\max}^{SPR}$ corresponding to n_e (P=0°) and n_0 (P=90°) is not as pronounced in the experimental data as seen in the simulations. We note that the achieved GNP volume fraction is very high in this composite. It is generally very difficult to obtain well-dispersed GNPs at high concentrations because of the large van der Waals attraction between GNPs. A recent study on GNP dispersion in organic solvents achieved volume fractions of the order of 10^{-3} [5]. In our smectic LC-GNP composite, however, the interaction between GNPs and the surrounding liquid crystal layered structure appears to prevent aggregation of GNPs even at rather high volume fractions [9]. This makes the smectic-GNP composite a highly promising material platform for novel metamaterial structures.

4. Conclusion

In conclusion, we have demonstrated the effect of an anisotropic medium on the surface plasmon resonance of the GNPs in LC-GNP dispersions. We have shown that the optical properties can be tuned by increasing the volume fraction of the GNPs. The observed dependence of the surface plasmon resonance wavelength on volume fraction of GNPs is in agreement with the effective medium theory. The realization of uniform dispersion of GNPs with high volume fraction enables the production of nanoparticle-based metamaterials, which provide an excellent alternative to nanolithographically fabricated metamaterials. While nanolithography tends to be slow and expensive, nanoparticle-based metamaterial can be fabricated by fast and cost-effective self-assembly methods. It is also straightforward to produce 3D metamaterial structures with nanoparticle dispersions, in contrast to the inherently 2D nature of lithographically fabricated structures. Extending our study to obtain stable dispersions of gold nanoparticles in ferroelectric smectic liquid crystals possessing inherent switching properties could enable tunable metamaterial architecture leading to interesting applications. Furthermore, the use of liquid crystal matrix automatically provides the possibility of dynamically tuning the metamaterial properties by external electric or optical fields, making the LC-GNP medium a highly promising metamaterial architecture.

Acknowledgements

This research was supported by the International Institute for Complex Adaptive Matter (ICAM-I2CAM), the NSF grants DMR-0844115, DMR-0820579 and DMR-0847782, the

#116095 - $15.00 USD Received 26 Aug 2009; revised 4 Oct 2009; accepted 4 Oct 2009; published 13 Oct 2009

Army Research Office (ARO) under Multidisciplinary University Research Initiative (MURI) contract 50432-PH-MUR and Office of Naval Research N00014-08-1-0874.

#116095 - $15.00 USD Received 26 Aug 2009; revised 4 Oct 2009; accepted 4 Oct 2009; published 13 Oct 2009